Electronic Supplementary Material (ESI) for Chemical Science.

Supporting Information for

Light Driven Mesoscale Assembly of a Coordination Polymeric Gelator into Flowers and Stars with Distinct Properties

Rahul Dev Mukhopadhyay,[ab] Vakayil K. Praveen,[a] Arpan Hazra,[c] Tapas Kumar Maji,[c] Ayyappanpillai Ajayaghosh*[ab]

---

[a] Photosciences and Photonics Section, Chemical Sciences and Technology Division,
CSIR-National Institute of Interdisciplinary Science and Technology (CSIR-NIIST),
Trivandrum, 695019, India.
Email: ajayaghosh@niist.res.in

[b] Academy of Scientific and Innovative Research (AcSIR),
CSIR-National Institute of Interdisciplinary Science and Technology (CSIR-NIIST),
Trivandrum, 695019, India.

[c] Chemistry and Physics of Materials Unit,
Jawaharlal Nehru Centre for Advanced Scientific Research (JNCASR),
Jakkur, Bangalore 560064, India.

Index

1. Materials and methods

1.1. Synthesis

Synthesis-general procedures. Unless otherwise stated, all starting materials, reagents and dry solvents were purchased from commercial suppliers and used as received. Azobenzene-4,4'-dicarboxylic acid (ADA) was synthesized according to Supplementary Scheme S1 based on a reported procedure.[S1]

Synthesis-characterization techniques. Melting points were determined with MEL-Temp-II melting point apparatus and are uncorrected. ^{1}H (500 MHz) and ^{13}C NMR (125 MHz) spectra were measured on a Bruker Avance DPX spectrometer. Chemical shifts are reported in parts per million (ppm) using tetramethylsilane (TMS) (δ_H = 0 ppm) or the solvent residual signal (DMSO-d_6: δ_C = 39.50 ppm) as an internal reference. FT-IR spectrum obtained from a Perkin-Elmer Spectrum One FT-IR spectrometer using KBr. Elemental analyses were performed with a Perkin-Elmer Series 2 Elemental Analyser 2400.

Synthesis and characterization of azobenzene-4,4'-dicarboxylic acid (ADA)

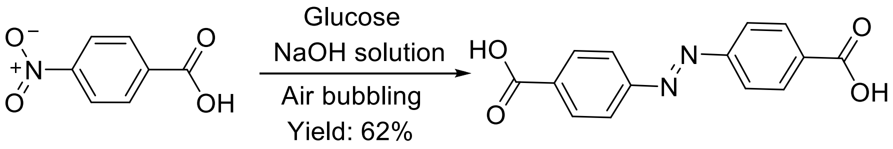

2 g of *p*-Nitrobenzoic acid and 6.7 g of sodium hydroxide were dissolved in 30 mL of distilled water by heating in a water bath. To this solution a solution of 13.33 g of glucose dissolved in 20 mL distilled water was added drop wise, maintaining the temperature of the water bath at 50 °C. The highly exothermic reaction results in the immediate formation of a dark brown solution. To this reaction mixture now a stream of air is passed with the help of a dropper fitted with a 5 W air pump.

The reaction mixture was kept in the water bath (50 °C) with constant air bubbling for 4-5 h and a chocolate brown precipitate was obtained. This was filtered and dissolved distilled water and later acidified by drop wise addition of glacial acetic acid resulting in a light pink precipitate. This precipitate was filtered and washed with plenty of water and then dried in an oven.

Yield: 62%; m.p. > 320 °C; FT-IR (KBr): ν_{max} = 2826(m), 1688(s), 1603(w), 1423(m), 1298(s), 933(m) cm^{-1}; ^{1}H NMR (500 MHz, DMSO-d_6, TMS, 25 °C): δ = 8.16 (d, 4H, Ar-*H*), 8.00 (d, 4H, Ar-*H*) ppm; ^{13}C NMR (125 MHz, DMSO-d_6, 25 °C): δ = 122.45, 130.31, 132.99, 153.78, 166.23 ppm; Elemental analysis: Calcd. for $C_{14}H_{10}N_2O_4$; C, 62.22; H, 3.73; N, 10.37. Found: C, 61.84; H, 3.60; N, 10.14.

Synthesis of nanoscale CPG1

100 mg of ADA dissolved in 50 mL of dry DMSO solvent is taken in a 250 mL amber color round bottom flask. To this solution 0.2 mL of triethyl amine is added and the flask is tightly stoppered and kept in an oil bath maintained at 50 °C for 2 h to confirm that the majority of the molecules remain in the thermodynamically favourable *trans* state. The temperature was then brought down to 40 °C and to this solution a solution of ferric nitrate nonahydrate (150 mg) in 50 mL dry DMSO was and the mixture was left undisturbed for 6-7 h. The temperature was slowly reduced to room temperature and the colloidal precipitate was collected via centrifugation. The material was purified by repeated cycles of washing and centrifugation.

Synthesis of nanoscale CPG2

For preparation of CPG2 100 mg of ADA dissolved in 50 mL of dry DMSO solvent added with 0.2 mL of triethyl amine was taken in a flat bottom quartz flask and irradiated with 365 nm light using a rayonet reactor for 2 h and to this solution ferric nitrate nonahydrate (150 mg) in 50 mL dry DMSO was and the mixture was left undisturbed for 6-7 h under UV light. It was verified that continuous irradiation did not increase the temperature of the reaction mixture to more than 40 °C. The material was purified by repeated cycles of washing and centrifugation.

In both case, a speck of the material was further dispersed in DMSO via sonication and then drop casted over freshly cleaved mica substrate for morphological analysis.

1.2. General procedures adopted

Time dependent SEM analysis was carried out by breaking the formed gel at different time intervals and dropcasting the same on freshly cleaved mica substrate. The samples were coated with gold prior to examination. The gel samples were washed with DMSO for several times to remove the excess starting materials. It was then dried in an oven, maintained at 150 °C for 24 h, to obtain the xerogel powder. The xerogel powder was used for TEM analysis, XRD, FT–IR and gas adsorption experiments. IFFT reconstruction of the HR-TEM images was done using a software programme, Digital Micrograph^{TM} (GATAN Inc.) following a reported procedure.[S2] Initially, a fast Fourier transform (FFT) of the experimentally obtained image was taken, which was followed by appropriate mask filtering to remove the spatial frequency of the diffrattogram. Finally, the Inverse FFT gave rise to a reconstructed HR-TEM image. Deconvolution of FT–IR spectra was performed using Fityk 0.9.8 software.[S3]

1.3. Measurements

Optical measurements and photoirradiation. Electronic absorption spectra were recorded on a Shimadzu UV-3600 scanning spectrophotometer using a 1 cm path length quartz cuvette. Solid-state absorption or reflection spectra were obtained using $BaSO_4$ as a standard. Photoirradiation was carried out by LOT-Oriel 200 W high pressure Hg Lamp using $\lambda_{\text{band pass}} = 350$ and 420 nm.

Morphological analysis. SEM images were obtained using a Zeiss EVO 18cryo SEM Special Edn with variable pressure detector working at 20-30 kV. Transmission electron microscopy (TEM) and high resolution TEM (HRTEM) were performed on a FEI, TECNAI 30 G2 S-TWIN microscope with an accelerating voltage of 100 and 300 kV, respectively. 1 mg of the samples of CPG1 or CPG2 (both purified and dried) were well dispersed in 5 mL methanol by ultra-sonication for 15 min and then dropcast on a carbon coated copper grids. Images were obtained without staining.

Rheology experiments. Rheological measurements were carried out in an Anton Paar Physical Modulated Compact Rheometre-150 Physica (Germany). A parallel plate sensor having a diameter 50 mm and a gap size of 0.1 mm was used. Measurements were carried out in dynamic oscillatory mode using strain amplitude of 1% in the frequency range 0.012-100 rad/sec.

BET adsorption studies. The BET adsorption isotherms for N_2 (at 77 K) and CO_2 (at 195 K) gases were performed in a QUANTACHROME QUADRASORB SI analyzer. About 100-125 mg of the xerogel samples (CPG1 and CPG2) were placed in sample cells, then the samples were outgassed under high vacuum condition at 423 K for 12 h in case of CPG1 and for 16 h in the case of CPG2 for N_2 adsorption and at 413 K for 10 h in case of CPG1 and 373 K for 5 h in case of CPG2 for CO_2 adsorption experiments. The adsorbate was taken in sample tubes and the change in pressure was monitored. The degree of adsorption was ascertained from the decrease in pressure at the equilibrium state. All operations were automatically performed and controlled by computers. Pore size distribution analysis was performed using the NLDFT equilibrium model.

2. Comparative FT-IR spectra of ADA, CPG1 and CPG2

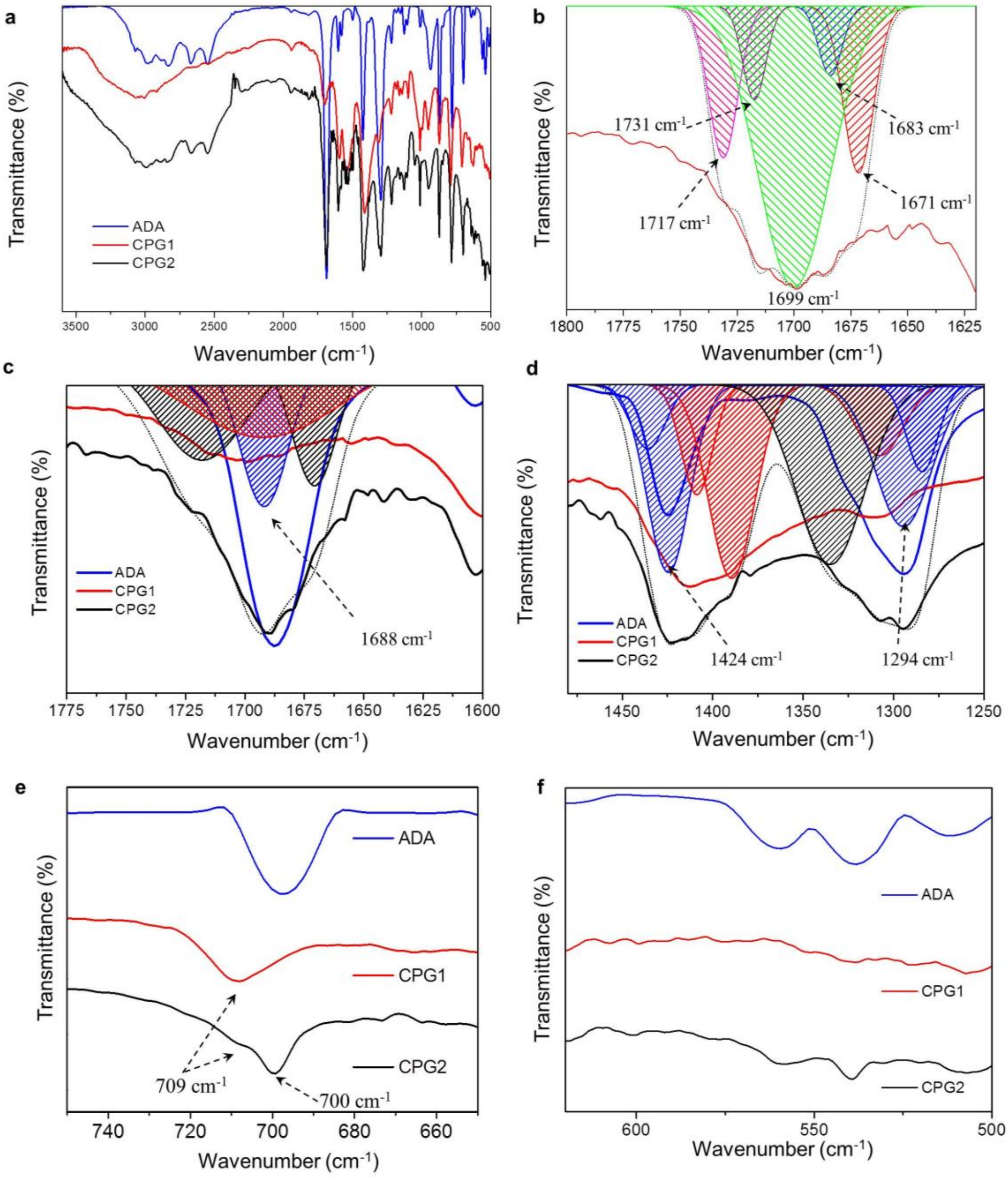

Fig. S1 (a) Comparative FT-IR spectra of ADA, CPG1 and CPG2. (b) Deconvolution of the broad assymmetric stretching frequency (~ 1700 cm^{-1}) band of CPG1 (shown in red). (c and d) Deconvolution of CPG2 FT-IR spectra shows the presence of both ADA as well as CPG1 peaks in CPG2. The shaded plots in all the above cases represent the functions obtained from the deconvolution of CPG1 and CPG2 spectra. The additive deconvoluted plot is represented in broken grey line in both cases. (e) Expanded portion of the region (750–650 cm^{-1}). Absence of band at ~720 cm^{-1} confirms that *cis* isomer of ADA is not present in CPG2. (f) Expanded portion of the region (620–500 cm^{-1}). Absence of band at ~560 cm^{-1} confirms that hematite phase is not present.

3. SEM images of CPG1 and CPG2

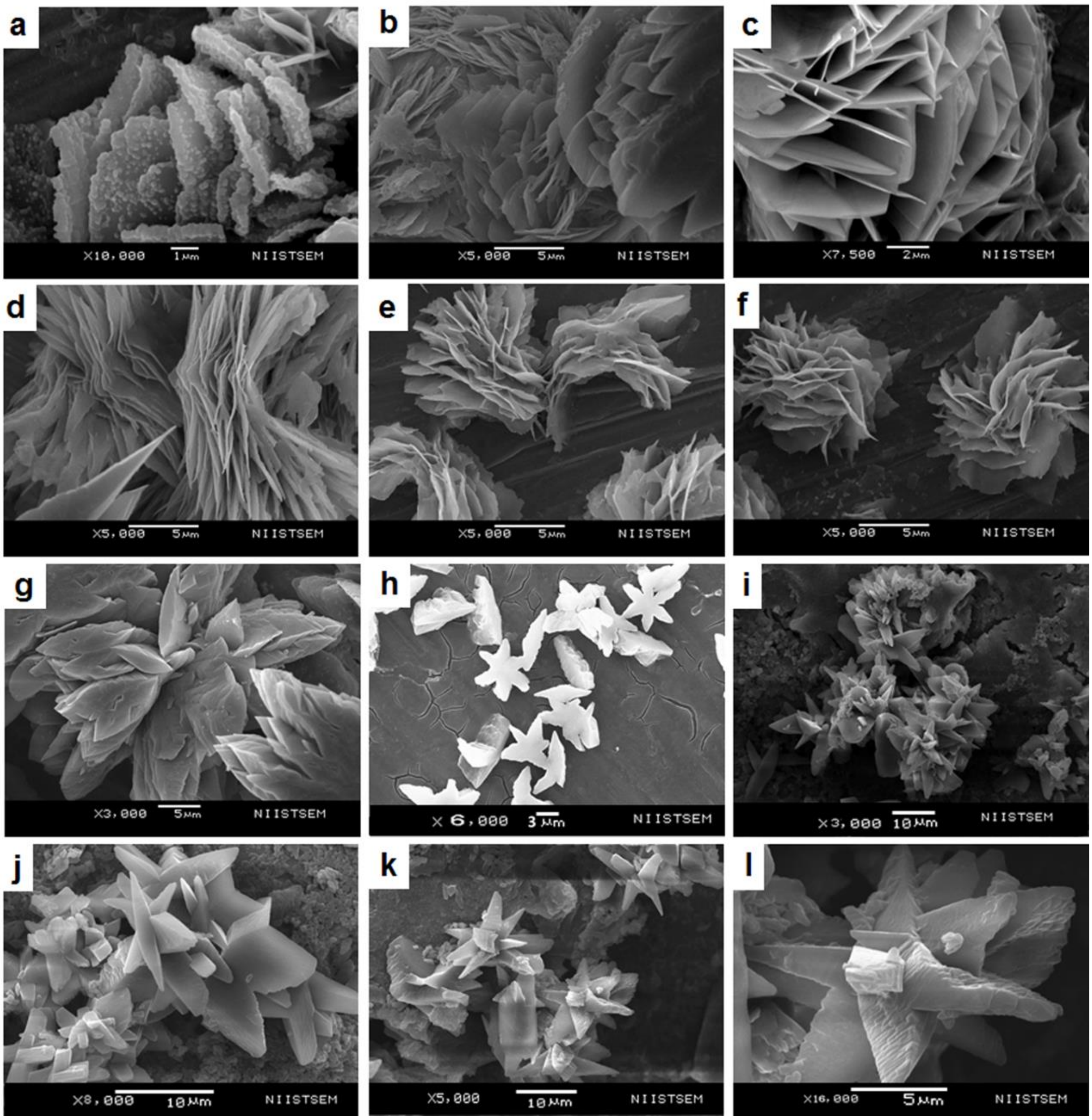

Fig. S2 SEM images of various hierarchical structures formed in case of (a-f) CPG1 and (g-l) CPG2. The formation of structures ranging from metal-organic flowers in case of CPG1 and metal-organic stars in case of CPG2 depends not only on time but also on local concentration.

4. TEM analysis of CPG2

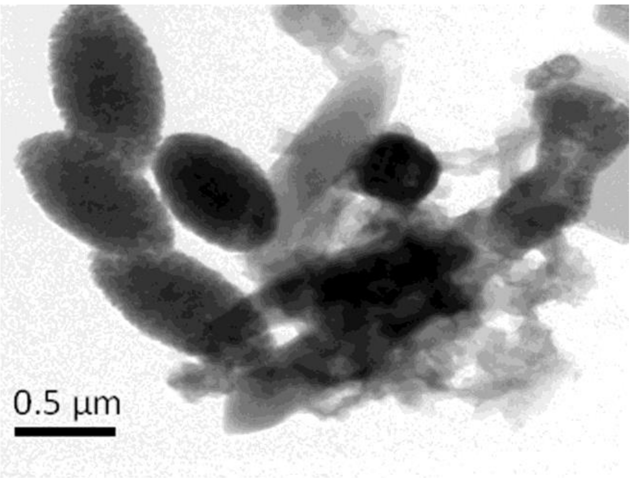

Fig. S3 TEM image of CPG2 displaying nano leaves and tentacles.

5. Diffusion limited kinetic assembly process

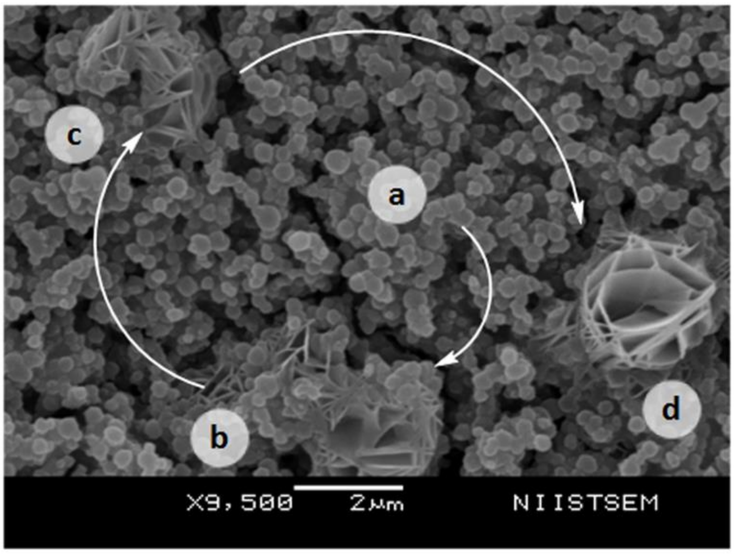

Fig. S4 SEM image of different stages in the formation of a cabbage structure captured in a single frame. The process might be taking place *via* (a) fusion of platelets, (b) small sheets with visible platelets, (c) gradual smoothening of rough sheets and (d) smooth sheets stacked to form a matured cabbage like structure.

6. Energy profile diagram

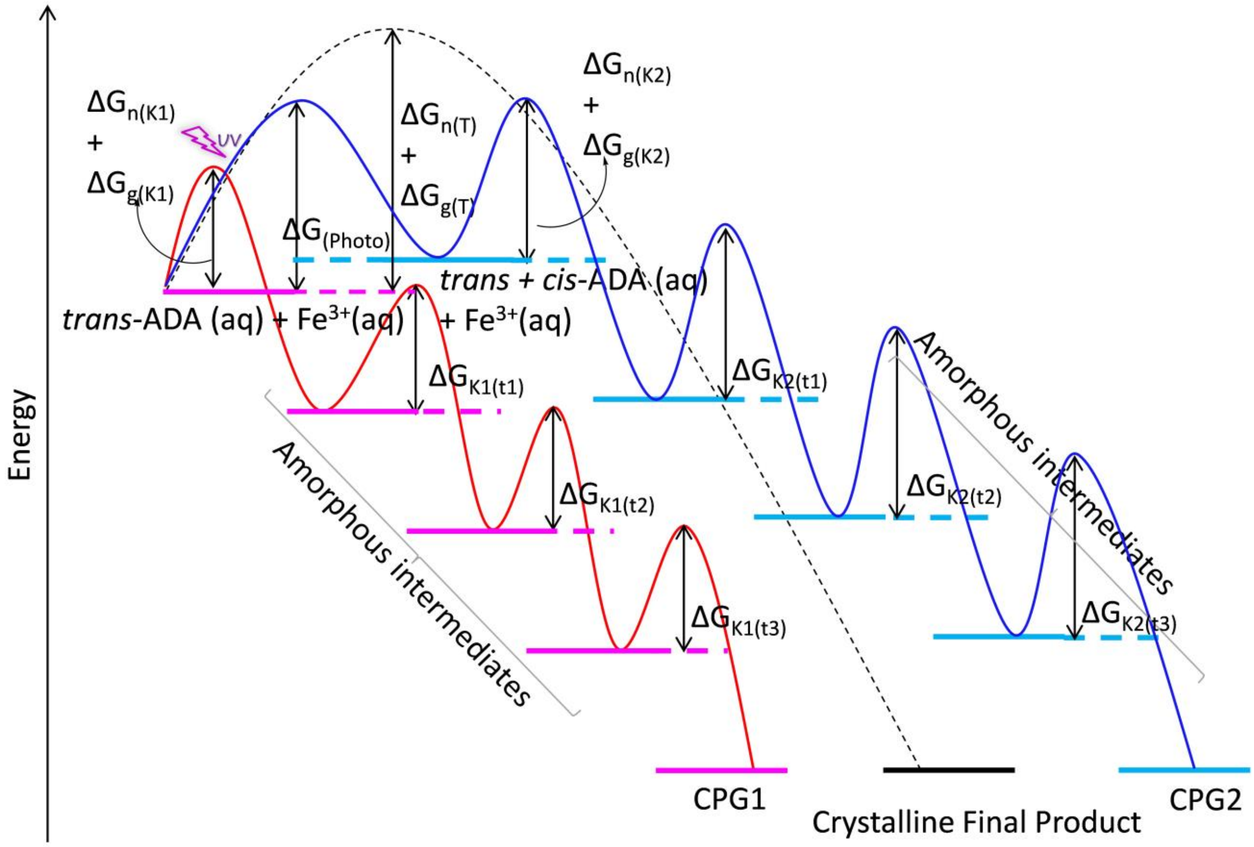

Fig. S5 Energy profile showing the thermodynamic and kinetic pathways of crystal growth. Thermodynamic (T) pathway is a one step process while kinetic (K1 and K2) pathways passes through several amorphous intermediate stages before ending up in a crystalline final product. The sequence of transformations depends on the free energy of activation of nucleation (ΔG_n), growth (ΔG_g) and phase transformations (ΔG_t). In case of photoirradiation at the beginning, there is additional activation energy for photoisomerisation (ΔG_{Photo}).

7. Nanoscale CPG particles obtained under thermodynamically controlled conditions

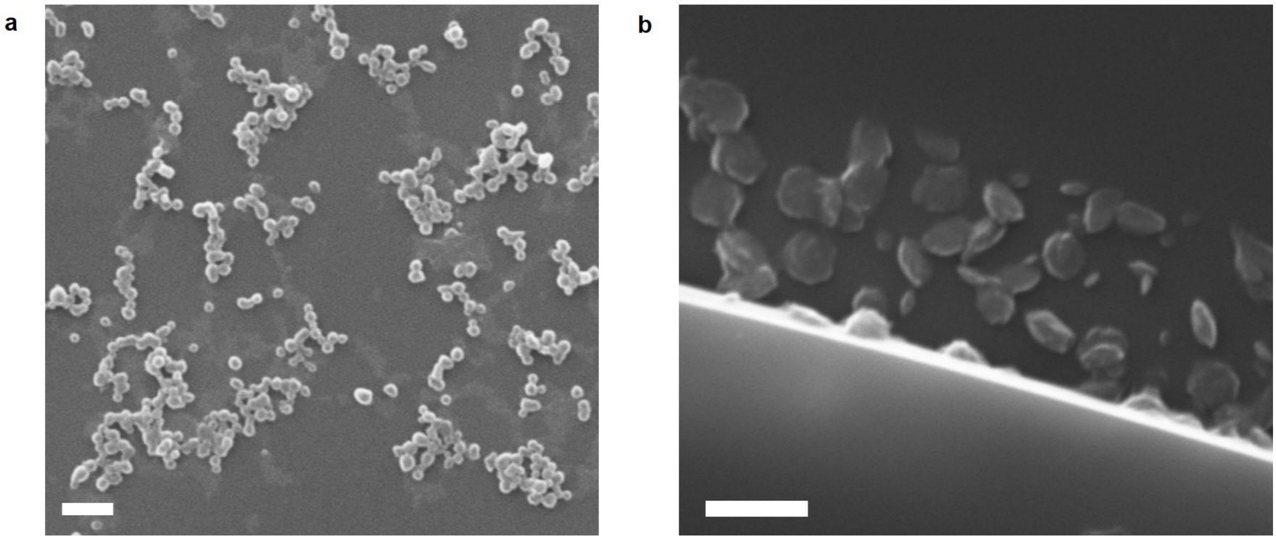

Fig. S6 Nanoscale coordination polymeric gel particles obtained under thermodynamic conditions. SEM images of (a) nanoscale CPG1 platelets, (b) nanoscale CPG2 leafs. Scale bar represents 1 µm.

8. Proposed formation mechanism for CPG1 and CPG2

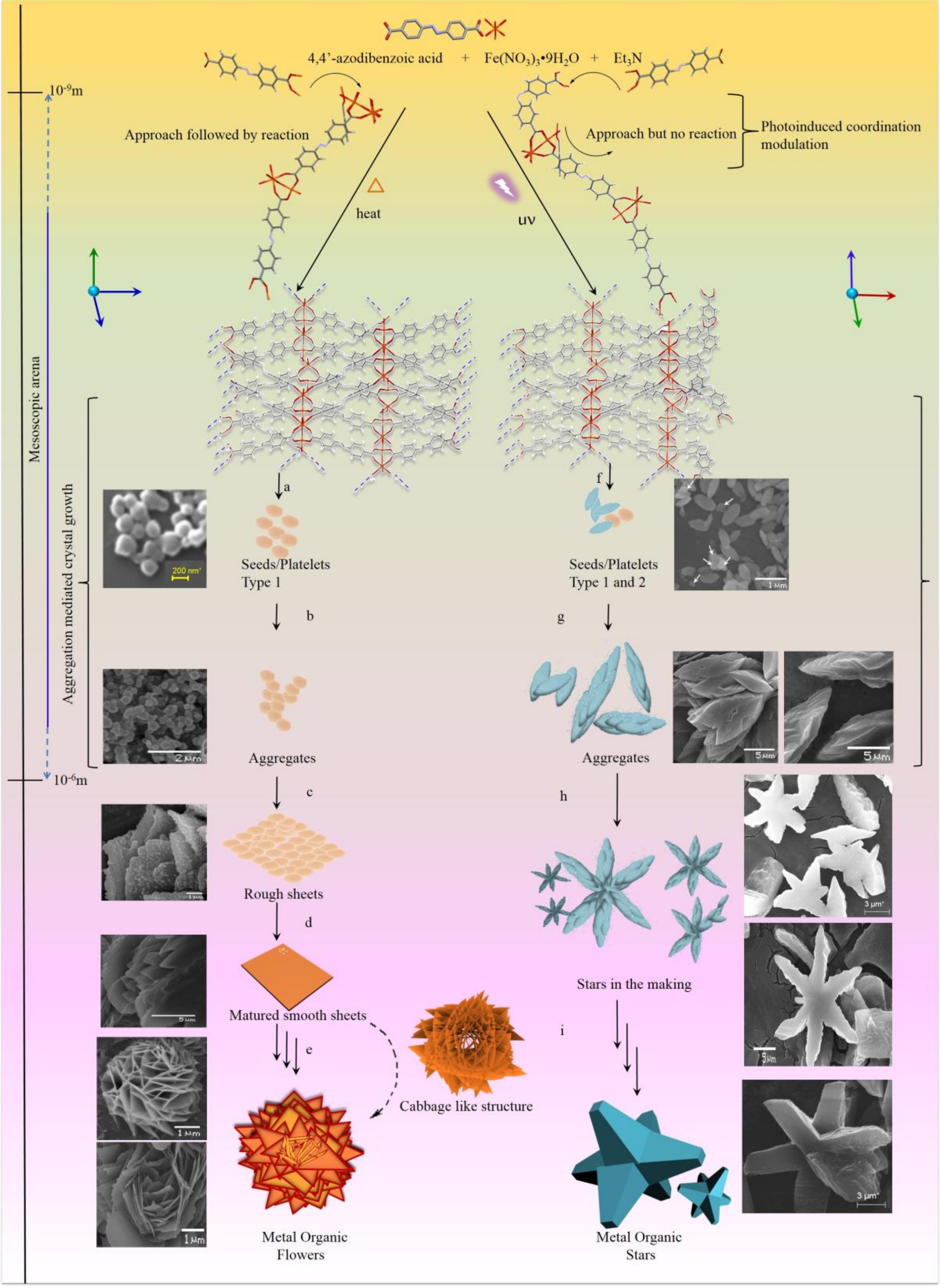

Fig. S7 (a and f) Nucleation, (b and g) aggregation, (c and h) fusion, (d) annealing, (e and j) culmination process leading to metal-organic flowers *via* cabbage like structure and metal-organic stars respectively. Blue, green and red arrows represent maximum, moderate and restricted rates of crystal growth. The SEM images representing different forms are cropped portions from experimentally obtained images are represented by appropriate scale bar. Blue broken lines indicate directions of polymeric extension.

9. Crystallographic view of PCN 243

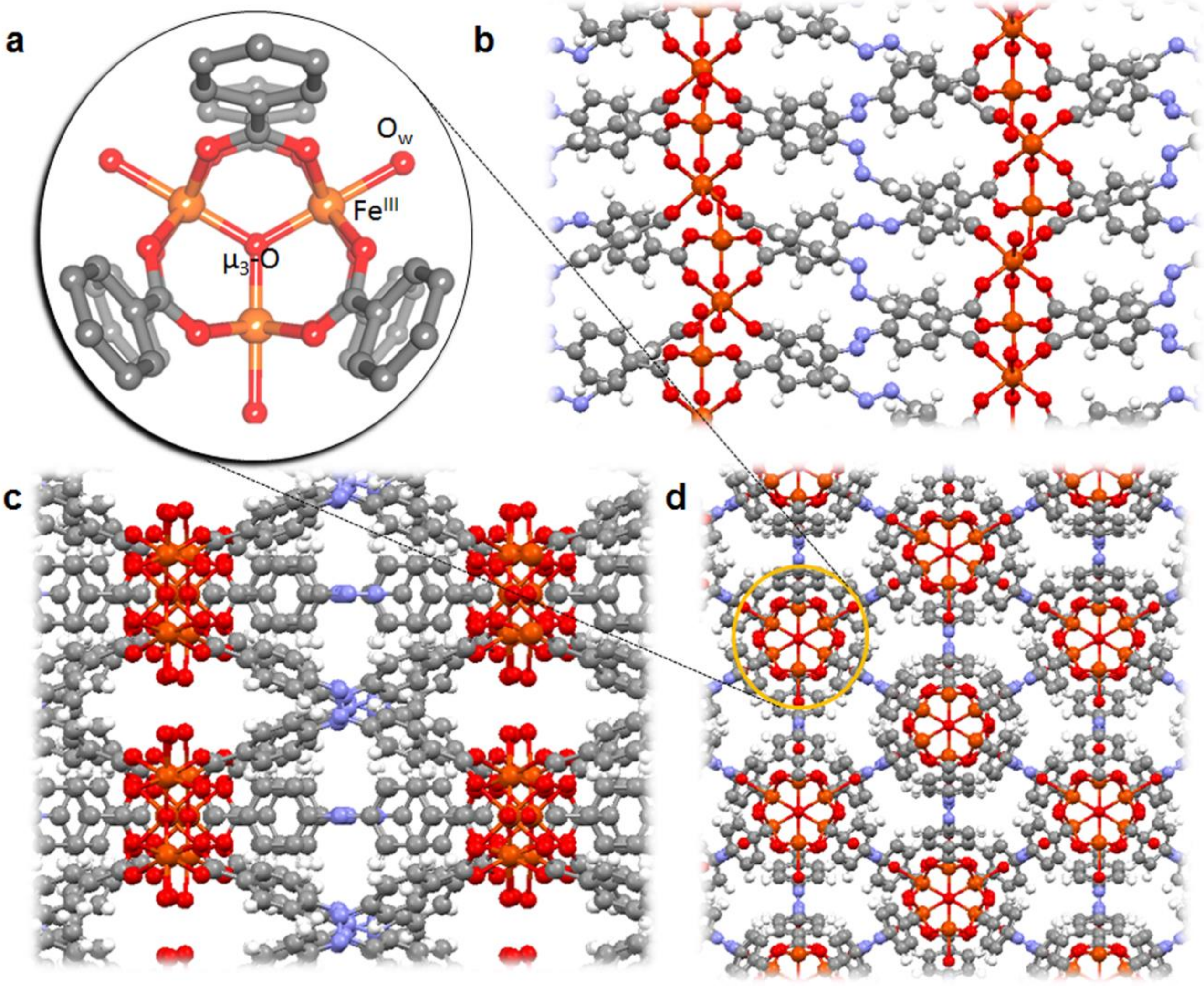

Fig. S8 (a) The fundamental building unit of PCN-243. Detailed view of the secondary building unit (SBU) containing the $[Fe_3(\mu_3\text{-}O)(COO)_6]$ cluster with coordinated solvent molecules (Ow). Each Fe^{III} center locates itself in a highly distorted octahedral environment. (b) View down the *b* axis. (c) View down the *b** axis. (d) View down the *c* axis.

10. EDX analysis

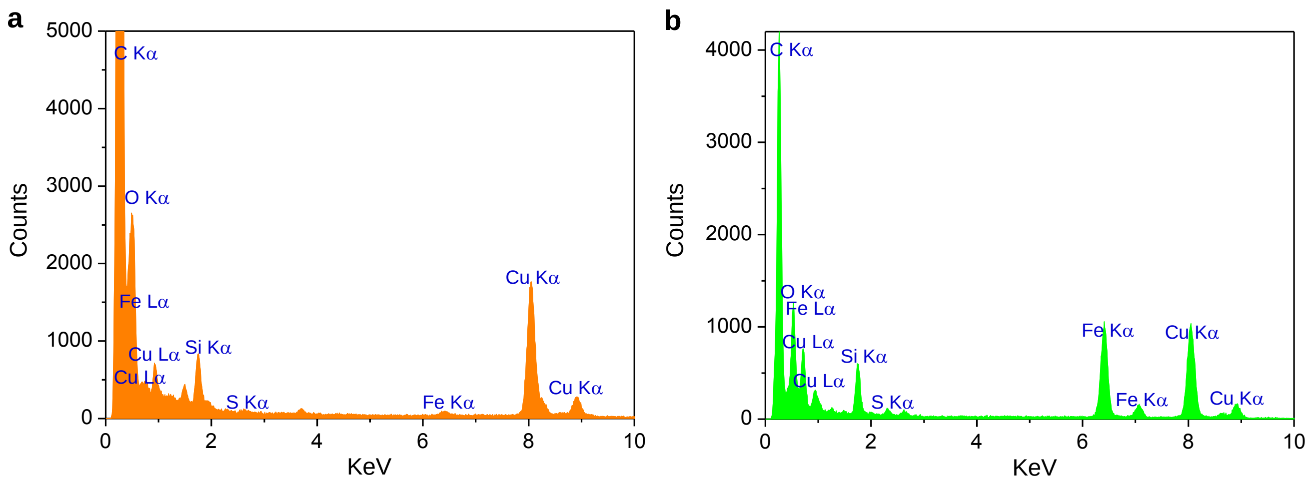

Fig. S9 EDX analysis of (a) CPG1 nanosheets and (b) CPG2 nanoleafs observed in TEM analysis.

11. Thermogravimetric analysis (TGA)

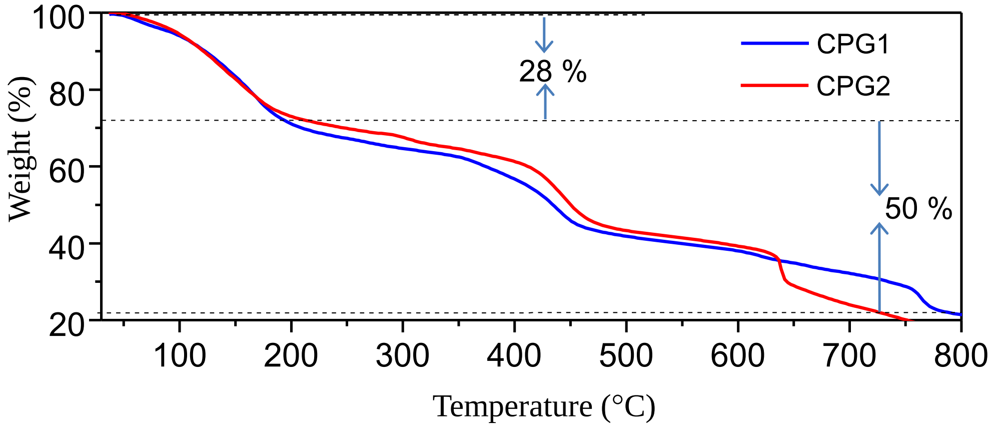

Fig. S10 Comparative TGA plot of CPG1 and CPG2.

12. Elemental analysis of CPG1 and CPG2

Experimentally obtained:

CPG1: Elemental analysis: C, 40.39; H, 3.96; N, 6.19; S, 8.16

CPG2: Elemental Analysis: C, 41.56; H, 4.31; N, 6.16; S, 8.57

13. Selected area electron diffraction (SAED) studies obtained from TEM analysis

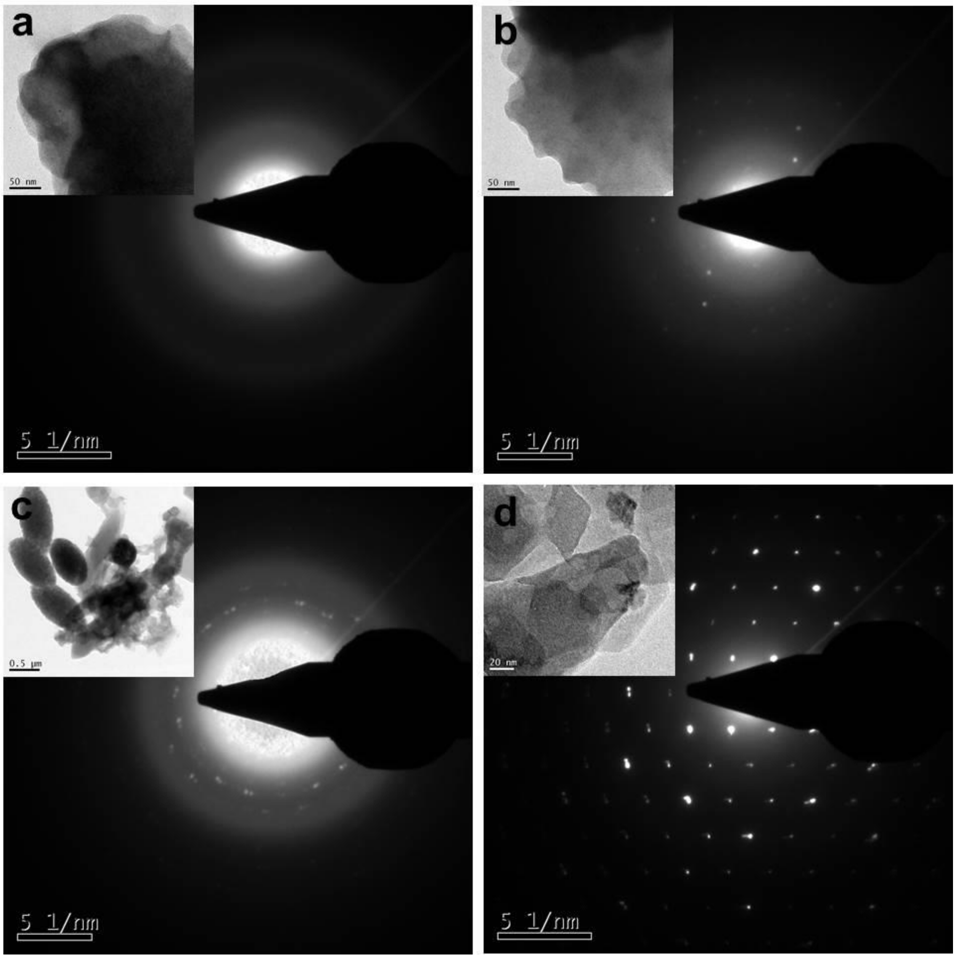

Fig. S11 SAED pattern obtained from (a and b) CPG1 and (c and d) CPG2. Insets show the respective TEM images. Amorphous (a) and partly crystalline pattern (b) was observed in CPG1 while polycrystalline (c) and single crystalline (d) pattern was observed in CPG2.

14. Control experiments with a gel forming non-photoresponsive organic ligand

Synthesis of FeBTC and irradiated FeBTC (IRFeBTC) gels

A solution of trimesic acid or 1,3,5-benzenetricarboxylic acid (BTC) in ethanol was mixed with an equal volume of $Fe(NO_3)_3•9H_2O$ in ethanol in 2:3 molar ratio resulting in immediate formation of FeBTC gel. For synthesis of IRFeBTC gel the ethanolic solution of BTC was irradiated with UV light ($\lambda_{\text{band pass}}$ = 350 nm) for 2 h prior to the addition of $Fe(NO_3)_3•9H_2O$ in ethanol.

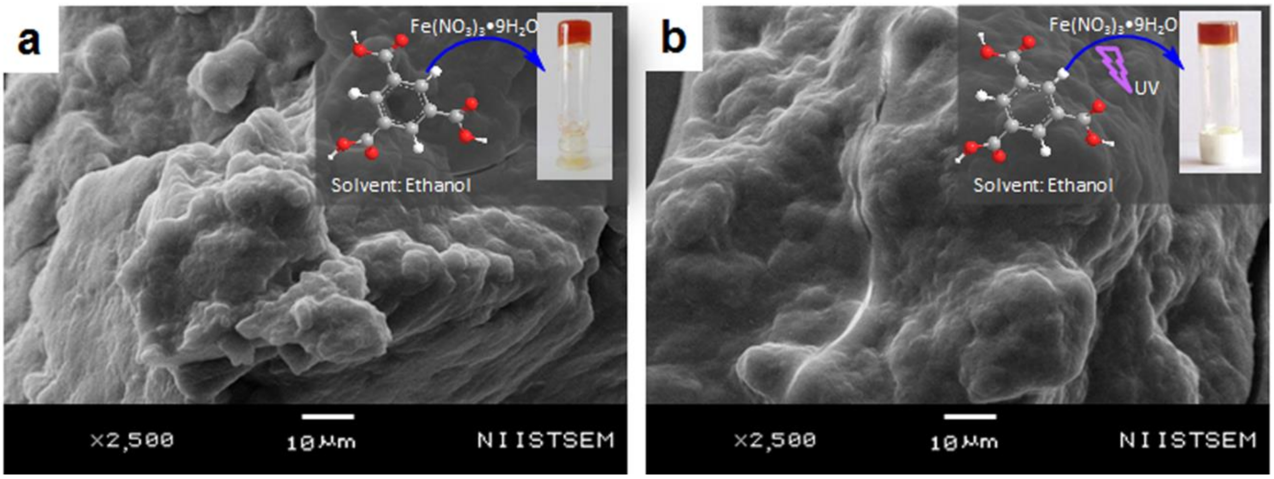

Figure S12. SEM images of (a) FeBTC gel and (b) IRFeBTC gel. No change in the morphology is observed in the two gel forms. Insets show the corresponding gel pictures along with the starting materials.

15. Pore-size distribution

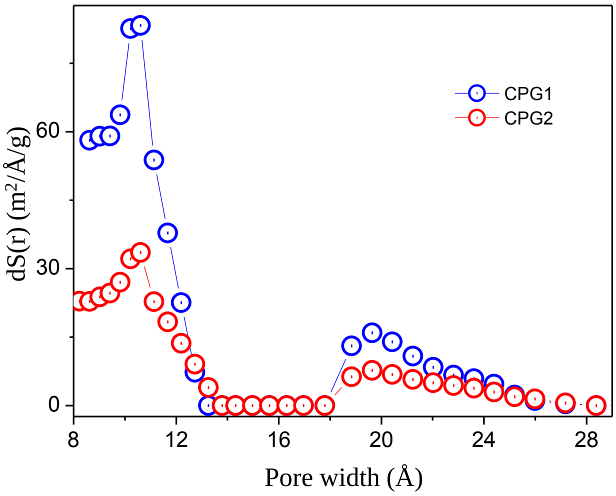

Fig. S13 Comparative pore size distribution for CPG1 and CPG2. Pore volume in CPG1 and CPG2 was calculated to be 0.127 and 0.062 cc/g, respectively

16. Comparison of difference in gas adsorption properties with previous literature reports

Table S1. Comparison of gas adsorption difference based on photoisomerisation of azobenzene.

Reference	**Maximum N_2 adsorption measured at 77 K for photoresponsive PCP with azobenzene in *trans* conformation**	**Maximum N_2 adsorption measured at 77 K for photoresponsive PCP with azobenzene in *cis* conformation**
S4	~ 5 cm^3 g^{-1}	~ 45 cm^3 g^{-1}

Table S2. Comparison of gas adsorption difference based on change in morphology of coordination polymers.

Reference	**Calculated BET surface area for elongated hexagonal coordination polymer particles (CPP6)**	**Calculated BET surface area for ellipsoidal coordination polymer particles (CPP7)**	**Calculated BET surface area for rod like coordination polymer particles (CPP8)**
S5	4.465 m^2 g^{-1}	4.492 m^2 g^{-1}	13.498 m^2 g^{-1}
	Maximum CO_2 adsorption measured at 195 K for elongated hexagonal coordination polymer particles (CPP6)	**Maximum CO_2 adsorption measured at 195 K for ellipsoidal coordination polymer particles (CPP7)**	**Maximum CO_2 adsorption measured at 195 K for rod like coordination polymer particles (CPP8)**
S5	~ 57 cm^3 g^{-1}	~ 60 cm^3 g^{-1}	~ 65 cm^3 g^{-1}

	Maximum N_2 adsorption measured at 77 K for CPG1 and BET surface area	**Maximum N_2 adsorption measured at 77 K for CPG2 and BET surface area**
Present work	88 cm^3 g^{-1}, 223 m^2/g	46 cm^3 g^{-1}, 90 m^2/g
	CO_2 adsorption measured at 195 K for CPG1 at relative pressure 0.03	**CO_2 adsorption measured at 195 K for CPG2 at relative pressure 0.03**
Present work	13 cm^3 g^{-1}	26 cm^3 g^{-1}

17. Photoisomerisation studies on CPG1 and CPG2 in the solid state

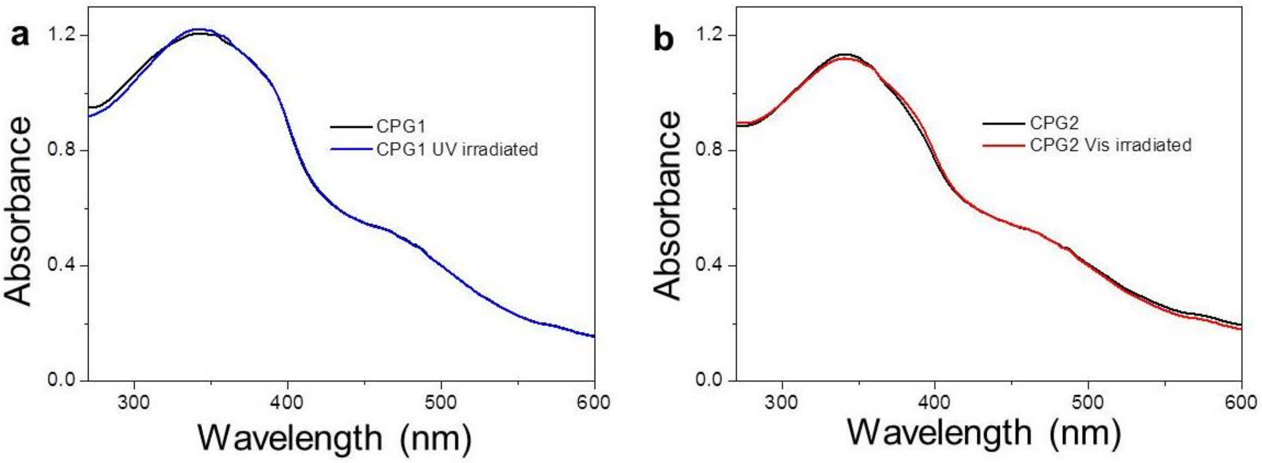

Fig. S14 (a) Changes in absorption spectrum of CPG1 with respect to UV light (350 nm) irradiation. (b) Changes in absorption spectrum of CPG2 with respect to visible light (420 nm) irradiation. Experiments were repeated after 1 h of irradiation in individual case.

18. Supporting references

S1. S. Ameerunisha and P. S. Zacharias, *J. Chem. Soc., Perkin Trans.*, 1995, **2**, 1679.

S2. Y.-M. Kim, J.-M. Jeong, J.-G. Kim, Y.-J. Kim and Y. S. Lim, *J. Korean Phys. Soc.*, 2006, **48**, 250.

S3. M. Wojdyr, *J. Appl. Cryst.*, 2010, **43**, 1126.

S4. N. Yanai, T. Uemura, M. Inoue, R. Matsuda, T. Fukushima, M. Tsujimoto, S. Isoda and S. Kitagawa, *J. Am. Chem. Soc.*, 2012, **134**, 4501.

S5. H. J. Lee, W. Cho, S. Jung and M. Oh, *Adv. Mater.,* 2009, **21**, 674.